https://doi.org/10.5194/egusphere-2025-5342
Preprint. Discussion started: 27 November 2025

Lacustrine methane release on the Tibetan Plateau as an important driver of Early Miocene global warming

Cheng Yang [1,2,3], Xiugen Fu [1,2,3,4*], Jinxian Deng [1,2,3*], Hengye Wei[1,2,3], Yue Wen[1,2,3], Tianxiang Wen[1,2,3], Shengqiang Zeng[5*]

[1] *School of Geoscience and Technology, Southwest Petroleum University, Chengdu 610500, China*

[2] *State Key Laboratory of Oil and Gas Reservoir Geologyand Exploitation, Southwest Petroleum University, Chengdu 610500，China*

[3] *Qiangtang institute of Sedimentary Basin, Southwest Petroleum University, Chengdu 610500, China*

[4] *Qinghai Provincial Key Laboratory of Plateau Saline-Lacustrine Basinal Oil & Gas Geology, Dunhuang 736202，China*

[5] *Chengdu Center, China Geological Survey (Geosciences Innovation Center of Southwest China), Chengdu 610218, China*

*Correspondence to: Xiugen Fu (fuxiugen@126.com), Jinxian Deng (448920726@qq.com), Shengqiang Zeng (zengsq@126.com)

Address: School of Geoscience and Technology, Southwest Petroleum University, Chengdu, 610500, China

https://doi.org/10.5194/egusphere-2025-5342
Preprint. Discussion started: 27 November 2025

Abstract. The Early Miocene was a key period of significant global warming. While previous studies often attributed this warming to the India-Asia collision and associated volcanism, an alternative mechanism may involve large-scale methane release from organic-rich lake sediments. To test the hypothesis that methane emissions from Tibetan Plateau lakes contributed to Early Miocene warming, we analyzed organic carbon, stable isotopes, and elemental concentrations in samples from the organic-rich Dingqinghu Formation in the Lunpola Basin, central Tibetan Plateau. Our results identify an exceptionally strong positive carbonate carbon isotope excursion ($\delta^{13}C_{carb}$ up to +13.79‰) within the lacustrine deposits. The large carbon isotope difference between carbonate and organic matter ($\Delta^{13}C$ > 32‰) indicates that methanogenesis, specifically via acetate fermentation, was the dominant microbial process. Extremely low sulfur contents likely suppressed sulfate-driven anaerobic oxidation of methane, facilitating direct methane release to the atmosphere. Furthermore, volcanic activity during this interval was limited, suggesting a negligible role in carbon cycle perturbations. The close temporal correspondence between Early Miocene warming, rising atmospheric CO_2, and methane emissions documented on the Tibetan Plateau indicates that methane release from these plateau lakes may have played an important role in driving global warming and increasing contemporary CO_2 levels.

https://doi.org/10.5194/egusphere-2025-5342
Preprint. Discussion started: 27 November 2025

1 Introduction

The Cenozoic era witnessed several global warming episodes, such the Paleocene-Eocene Thermal Maximum and the Middle Miocene Climatic Optimum, with temperatures and atmospheric CO_2 concentrations significantly exceeding pre-industrial levels (Methner et al., 2020; Cenozoic CO2 Proxy Integration Project (CenCO2PIP) Consortium, 2023; Ivany et al., 2025). This period was also defined by continental collision between India and Eurasia and the subsequent uplift of the Tibetan Plateau, a tectonic event that profoundly reshaped Asian climate and potentially influenced global patterns (Wang et al.,2008; Yang et al.,2022; Zhang et al.,2024; Zhang et al.,2025). The temporal coincidence of these events has led to the hypothesis that the India-Asia collision and its associated volcanism may have been a primary driver of Cenozoic warming (Gutjahr et al., 2017; Kender et al., 2021; Tremblin et al., 2022).

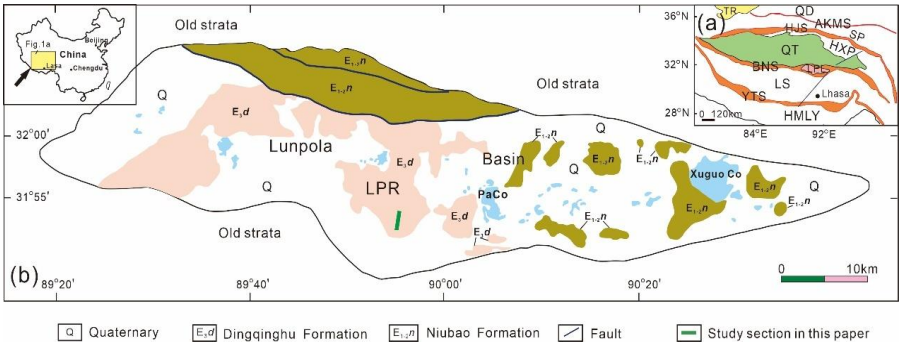

Figure 1:(a) Map of the Tibetan plateau showing major terranes. (b) Simplified geological map of the Lunpola Basin, showing location of sampling section. AKMS, Anyimaqen–Kunlun–Muztagh Suture; BNS, Bangong Lake–Nujiang River Suture; HJS, Hoh Xil–Jinsha River Suture; HMLY, Himalayas; HXP, Hoh Xili piedmont zone; LPL, Lunpola Basin; LS, Lhasa terrane; QD, Qaidam; QT, Qiagtang Basin; SP, Songpan–Ganzi flysch complex; TR, Tarim Basin; YTS, Yarlung Tsangpo Suture（modified from Fu et al,2015）.

However, Cenozoic volcanism on the Tibetan Plateau, while episodic, was relatively limited in scale (Xie et al., 2024). For instance, during the third volcanic phase (ca. 28–18 Ma), activity was largely confined to restricted areas like the Lunpola Basin, with

https://doi.org/10.5194/egusphere-2025-5342
Preprint. Discussion started: 27 November 2025

significantly reduced spatial distribution and magma volume compared to earlier stages (Wang et al., 2024). Consequently, although regional magmatic events reflect the tectonic-magmatic evolution of the Plateau, their associated volatile fluxes were likely negligible on a global scale compared to large igneous provinces (Zhang et al., 2021). This suggests that the direct contribution of Tibetan volcanism to the rise in atmospheric CO_2 and global warming was probably limited.

An alternative mechanism for driving warming may involve large-scale methane release from organic-rich lake sediments. During diagenesis and burial, microbial methanogenesis in such sediments can generate substantial methane (CH_4) (Martens and Berner, 1974; Whiticar, 1999; Bastviken et al., 2004; Dean et al., 2018). Under stratified or anoxic lacustrine conditions, this methane can accumulate and be released to atmosphere via ebullition and diffusion (Bastviken et al., 2004; Encinas Fernández et al., 2014; DelSontro et al., 2016). Lakes are a significant natural source of methane emissions, and during specific geological intervals, widespread organic-rich lacustrine systems could have release methane at a scale capable of influencing the global climate system by enhancing the greenhouse effect and perturbing the carbon cycle (Dean et al., 2018; Sun et al., 2022; Zhuang et al., 2023). Consequently, organic-enriched lake sediments act not only a crucial long-term carbon sink but also, under certain conditions, as a potent methane source, with substantial implications for both paleoclimate and contemporary climate system.

During the Miocene, the Tibetan Plateau hosted extensive lacustrine systems. The Lunpola and Nima basins, for example, preserve thick successions of organic-rich deposits and oil shales. In the Dingqinghu Formation, these successions reach thicknesses exceeding 148 m and exhibit total organic carbon (TOC) contents of up to 17.60% (Fu et al.,2012; Fang et al.,2020; Fu et al.,2020; Lu，2023；Zeng et al., 2024). These deposits not only record high organic carbon accumulation but also represent a potential source of large methane emissions during deposition and early diagenesis, which could have contributed to regional or even global warming (Zhou et al., 2024;

https://doi.org/10.5194/egusphere-2025-5342
Preprint. Discussion started: 27 November 2025

Nie et al., 2023).

To test the hypothesis that methane release from Tibetan Plateau lakes contributed to Early Miocene warming, we conducted organic carbon, stable isotope, and element analyses on samples from the Dingqinghu Formation in the Lunpola Basin (Fig. 1a). Integrated with a robust chronological framework (Mao et al., 2019), this multi-proxy dataset allows us to correlate regional geological events with global climate records and evaluate the potential mechanisms driving Early Miocene climate warmi

2 Geological setting

The Lunpola Basin is a Cenozoic fault-depression basin located on the central Tibetan Plateau, within the central segment of the Bangong-Nujiang Suture Zone (BNSZ), a major tectonic boundary separating the Lhasa and Qiangtang terranes. The basin extends approximately 200 km from east to west and 10-30 km from north to south, and is recognized as the highest-altitude petroleum-bearing basin in the world (Deng et al., 2012; Rowley & Currie, 2006; Fu et al., 2012; Wang et al., 2025).

The Tibetan Plateau comprises a series of east-striking tectonic units bounded by major suture zones. From north to south, they are the Kunlun-Qaidam Terrane, the Songpan-Ganzi flysch complex, the Qiangtang Terrane, and the Lhasa Terrane, separated by the Anyimaqen-Kunlun-Muztagh, Hoh Xil-Jinsha River, and Bangong Lake-Nujiang River (BNS) suture zones, respectively (Fig. 1a). The BNS originated from the diachronous, west-to-east closure of the Meso-Tethyan ocean basin, culminating in the Late Jurassic–Early Cretaceous Lhasa-Qiangtang collision (Kapp and DeCelles, 2019). It was later reactivated during contractional events in the latest Cretaceous and Oligocene–early Miocene, which led to the development of intermontane basins in central Tibet, including the Lunpola, Nima, and Gerze basins (e.g., Wei et al., 2017; Han et al., 2019).

Structurally, the basin is influenced by strike-slip and thrust faulting, forming a pod-like framework characterized by “north–south structural zoning and east–west fault blocking.” In the north–south direction, the basin exhibits high flanks and a central

https://doi.org/10.5194/egusphere-2025-5342
Preprint. Discussion started: 27 November 2025

depression. The southern margin is controlled by thrust belts and uplifts, while the northern part shows localized highs despite significant subsidence and thick sedimentary infill. The cumulative thickness of the Niubao and Dingqinghu formations exceeds 3,000 m. East–west segmentation by faults results in a pattern of peripheral uplift and central subsidence (Lei et al., 1997).

The tectonic evolution of the Lunpola Basin involved two main stages. The Eoc[illegible] rifting, during which the Niubao Formation ($E_{1-2}n$) was deposited, consisting mainly of alluvial fan to fan-delta coarse clastics. The Oligocene depression, marked by accumulation of the Dingqinghu Formation (E_3d), dominated by deep lacustrine fine-grained mudstones and oil shales (Deng et al., 2012; Lu, 2023). The Dingqinghu Formation is distributed primarily in the central and western parts of the basin, with thickness varying from 300 to 1,100 m due to differential basement subsidence. It comprises greenish-gray shales, mudstones, and oil shales interbedded with thin sandstones, interpreted as having been deposited in a low-energy, semi-deep to deep lacustrine environment under stable and strongly reducing conditions (Fu et al., 2015). This study focuses on the middle member of the Dingqinghu Formation, which is Early Miocene in age (ca. 20.6 ± 0.1 Ma; Mao et al., 2019) and consists of organic-rich mudstones, shales, and oil shales. These oil shale samples are dark brown to black in color and contain high organic matter content.

3 Method

The study area and section location are presented in Fig. [illegible]. The vertical distribution of samples within the section is presented in Figs. S1. A total of 63 samples were collected from the Lunpola oil shale section. The average vertical sampling interval is 60 cm.

3.1 TOC analysis

First, grind the 10 mg rock sample into a powder with a particle size smaller than 200 mesh. Then, depending on the lithology and colour of the sample, 0.095–0.105 g of the

https://doi.org/10.5194/egusphere-2025-5342
Preprint. Discussion started: 27 November 2025

powdered rock is weighed into a crucible and placed into the container. Slowly add 10% HCl along the inner wall of the container (ensuring it does not overflow the crucible opening), then allow it to decarburise for over 24 hours until the reaction is complete. Remove the crucible, rinse the sample with high-purity water to wash away residual acid, and continue washing until the rinse water is neutral. After washing, the samples were dried in an electric thermostatic drying oven at 60–80°C and then analysed for TOC content using an LDH CS analyser (Model: TK851-6K) at the Qiangtang Institute of Sedimentary Basin, Southwest Petroleum University. For every 10 samples, a parallel sample was included for quality control. Results were recorded in wt%, with an analytical accuracy better than ±0.1‰.

3.2 Inorganic carbon and oxygen isotope analysis

Carbon isotope samples were analysed in the laboratory of the Qiangtang Institute of Sedimentary Basin. First, an appropriate amount of carbonate sample was ground with an agate mortar to less than 200 mesh, then dried in an oven at 60℃ for approximately 4 hours to remove adsorbed water. Then, approximately 1 mg of the sample was placed into the sample tube of the GasBench Plus sample preparation system. The sample was dried at 70℃, the tube was sealed, and the air in the sample tube was purged with high-purity helium (He). Using an acid pump with an acid needle, excess 100% phosphoric acid (H_3PO_4) was added to the sample tube. The phosphoric acid was allowed to react with the carbonate sample to produce CO_2 gas. The generated CO_2 was then carried by high-purity helium into the Delta Q (Thermo Fisher) system, where the carbon and oxygen isotopic compositions were measured. A standard reference material was analysed after every 12 samples for quality control. Results were reported in $\delta^{13}C$ V-PDB and $\delta^{18}O$ V-PDB values relative to the PDB standard. The GB04416 carbonate standard yielded $\delta^{13}C$ =1.67 ± 0.05‰, and measurement accuracy was ±0.05‰. For carbonate samples, analytical reproducibility of replicate standards was better than ±0.07‰.

https://doi.org/10.5194/egusphere-2025-5342
Preprint. Discussion started: 27 November 2025

3.3 Organic carbon isotope analysis

The whole rock powder sample was decarbonised with 10% HCl for 48 hours to eliminate all carbonate components, then washed with ultra-pure water until neutral, and the residual sample was dried, ground to less than 200 mesh, weighed 0.2 to 5 mg of residual powder sample into a tin cup, and tightly wrapped into cubes. Under the He atmosphere, the gas is sent into the high-temperature oxidation tube through the EA auto-sampler and instantly oxidised at 980℃ in an oxygen atmosphere to generate a mixture of various gas components such as NO, N_2O, N_2O_2, N_2, CO, CO_2, H_2O, SO_2 and halogen. In the reaction tube, CO is oxidised to CO_2 by chromium oxide and silver-coated cobalt oxide, and SO_2 and halogen gases are removed. Subsequently, in a reduction tube at 650°C, copper wire reduces nitrogen oxides to N_2 and absorbs excess O_2. The resulting helium and carbon dioxide gases pass through a magnesium perchlorate chemical trap to remove moisture, and then are separated by a chromatographic column into N_2 and CO_2, which enter a thermal conductivity detector (TCD) to determine the carbon content. A small amount of CO_2 is then introduced into a connected Delta Q mass spectrometer via a continuous flow ConFIV system to measure the isotope ratio. All carbon isotope values are reported in the conventional δ -notation in per mil relative to V-PDB (Vienna-PDB). The accuracy and reproducibility of the analysis were checked through repeated tests of the international standard sample USGS40, and the accuracy (1σ) was less than 0.09‰. The repeatability test accuracy of the sample is less than 0.13‰.

3.4 Total nitrogen (TN) and nitrogen isotope ($\delta^{15}N$)

The total nitrogen (TN) and nitrogen isotope ($\delta^{15}N$) contents of samples were measured at Qiangtang Institute of Sedimentary Basin, Southwest Petroleum University, China, using a Vario Macro Cube elemental analyser (Elementar, Hanau, Germany). Approximately 200 mg of the powder samples were weighed, and then add 50 mg of WO_3 oxidant. The mixture was tightly enclosed with a 35 × 35 mm tin capsule and prepared for analysis. Standard deviations for carbon, nitrogen and sulfur contents are

https://doi.org/10.5194/egusphere-2025-5342
Preprint. Discussion started: 27 November 2025

202 <0.05 wt% (1σ) based on replicate analyses of multiple samples. Thus, the analytical
203 precision of TN measurements was always better than 0.05 wt.%.

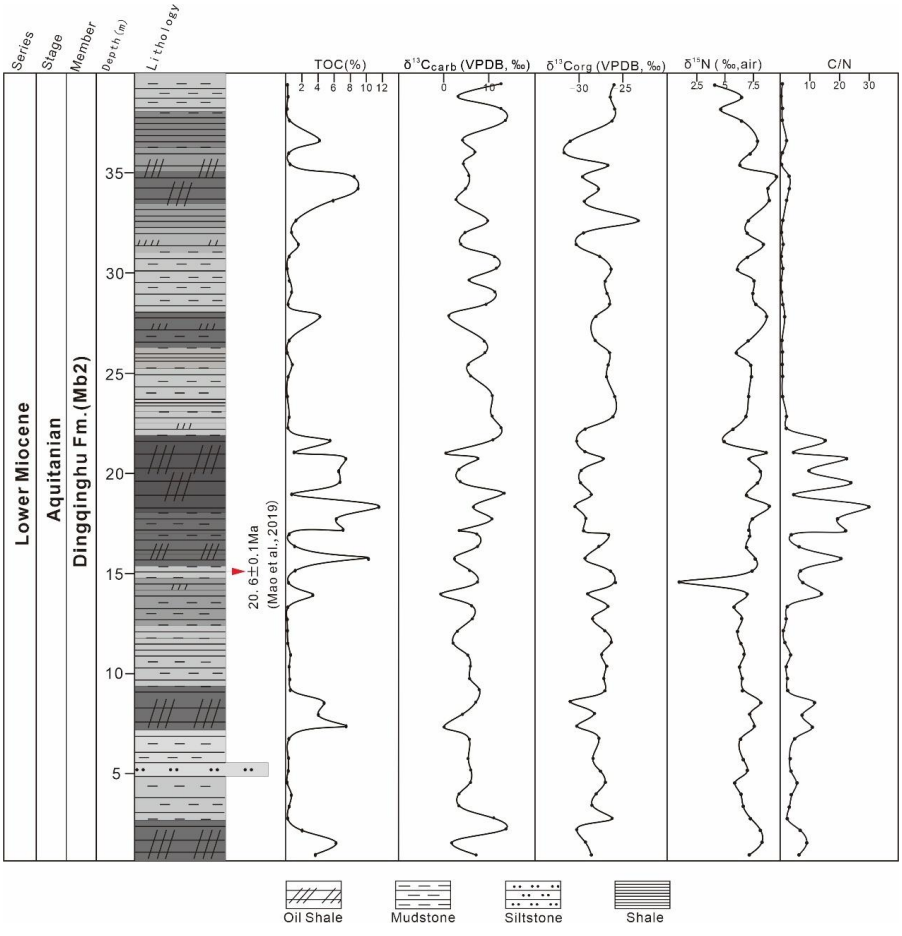

204

205 Figure 2: TOC, $\delta^{13}C_{carb}$ (the Carbonate carbon isotope), $\delta^{13}C_{org}$ (the Organic Carbon Isotope), $\delta^{15}N$
206 (the Organic Nitrogen isotope) and C/N ratio data in Dingqinghu Formation of lunpola basin.

207 *3.5 The major elements and trace elements*

208 Elemental analyses were conducted at the Qiangtang Basin Research Institute,
209 Southwest Petroleum University. Powdered samples (<200 mesh) were packed into
210 Chemplex cups, compacted, and sealed with polypropylene film. Major and selected
211 trace element concentrations (including Ca, Mg, Ba, Cu, Ni, V and Sr) were measured
212 using a Bruker S1 TITAN 800 X-ray fluorescence (XRF) spectrometer manufactured

https://doi.org/10.5194/egusphere-2025-5342
Preprint. Discussion started: 27 November 2025

by Bruker, Germany. The standard deviation for major elements was better than ± 0.05%, and that for trace elements was better than ±20 μg/g.

4 Result

4.1 TOC content

The total organic carbon content of mudstone and oil shale samples from the Second Member of the Dingqinghu formation is illustrated in Fig. 2. The TOC values exhibit a wide variation range (0.12%-11.54%), with an average of 2.35%, categorizing these strata as high-quality source rocks. Notably, the oil shale intervals demonstrate exceptional organic enrichment, characterized by TOC values spanning 0.56%-11.54%, with an average of 5.37%, which exceeds the threshold for effective hydrocarbon generation in lacustrine systems. In contrast, the interbedded mudstones and shales display comparatively lower TOC concentrations, ranging from 0.12% to 7.36%, with an average of 0.91%.

4.2 Stable Isotope geochemistry

As shown in Fig. 2, the variations of $\delta^{13}C_{carb}$ values of the second member of the Dingqinghu formation exhibit an extreme positive excursion, ranging from -0.84‰ to 13.79‰, with an average of 6.59‰. The variation curve of $\delta^{13}C_{carb}$ values reveals that mudstone intervals display the most pronounced positive excursion (1.23‰–13.67‰, averaging 7.39‰), while oil shale intervals show relatively lower values (-0.84‰–13.79‰, averaging 4.91‰).The $\delta^{13}C_{org}$ values of the Second Member of the Dingqinghu Formation range from -31.64‰ to -23.31‰, with an average value of -27.97‰. The $\delta^{13}C_{org}$ curve demonstrates a negative excursion in the oil shale layers, where values vary between -31.03‰ and -26.76‰ (average: -29.34‰). In contrast, the mudstone intervals exhibit a positive excursion, with a broader $\delta^{13}C_{org}$ range of -31.64‰ to -23.31‰ and an average of -27.33‰. The curves of $\delta^{13}C_{carb}$ and $\delta^{13}C_{org}$ exhibit high coupling, which reflect the synergistic response mechanism of lake carbon cycle and climate environment. The organic nitrogen isotope values ($\delta^{15}N$(‰,air)) of

https://doi.org/10.5194/egusphere-2025-5342
Preprint. Discussion started: 27 November 2025

the Second Member of the Dingqinghu Formation range from 1.06‰ to 9.74‰, with an average value of 7.11‰.

5 Discussion

5.1 Influence of modifying factors

Since both carbonates and organic matter can preserve diagenetic information rather than primary depositional signals after sedimentation, the influence of diagenesis must be evaluated prior to interpreting the isotopic compositions. Following precipitation in lake water bodies, carbonate minerals undergo a series of diagenetic alteration processes during burial, influenced by temperature and pore fluids. These processes, including dissolution and recrystallization, can lead to isotopic re-equilibration between the minerals and fluids (Boever et al., 2017; Hillaire et al., 2021; Huntington and Petersen, 2023). The extent of diagenetic alteration in lacustrine sediments can be assessed using carbon and oxygen isotopes of carbonate minerals. During diagenesis, carbon in pore fluids is typically scarce relative to the reservoir within carbonates, resulting in a rock-buffered system for carbon. Conversely, oxygen is predominantly soured from pore fluids, creating a fluid-buffered system for oxygen. Consequently, oxygen isotopic compositions are highly susceptible to alteration during diagenesis, while carbon isotopic compositions generally remain more resistant to change (Wang, 2008; De Boever et al., 2017; Horacek et al., 2007; Ritter et al., 2017; Huntington and Petersen, 2023). The correlation between carbonate $\delta^{13}C_{carb}$ and $\delta^{18}O$ values can therefore be utilized to assess the degree of diagenetic influence on carbon isotopes. In the present study, the $\delta^{13}C_{carb}$ vs. $\delta^{18}O$ plot (Figs. S2a) exhibits a weak correlation (R^2=0.0132), indicating that the $\delta^{13}C_{carb}$ values retain primary depositional signals. Furthermore, the Mn/Sr ratio, a sensitive indicator of post-depositional alteration (Hu et al., 2023), show no significant correlation with either $\delta^{13}C_{carb}$ (R^2=0.0012, Figs. S2b) or $\delta^{13}C_{org}$ (R^2=0.017, Figs. S2c). These results collectively suggest a negligible influence of diagenesis on the measured carbon isotopic signatures.

Diagenetic and metamorphic processes can significantly alter the $\delta^{15}N$ values of lake

https://doi.org/10.5194/egusphere-2025-5342
Preprint. Discussion started: 27 November 2025

sediments. During diagenesis, microbial decomposition releases ^{14}N-enriched NH^{4+} into the pore water, resulting in ^{15}N enrichment of residual organic matter and more positive ^{15}N values (Macko et al., 1987; Altabet, 1988; Lourey etal., 2003; Papineau et al., 2009). Metamorphic processes similarly affect ^{15}N through thermal degradation of nitrogen-rich compounds, which preferentially releases ^{14}N-enriched NH_3 or N_2, leaving residual organic matter with elevated ^{15}N values (Freudenthal et al., 2001; Lehmann et al., 2002; Altabet, 2006; Robinson et al., 2012; Stüeken et al., 2016; Xia et al., 2022). Correlative relationships among TOC, TN, $\delta^{13}C_{org}$ and $\delta^{15}N$ serve as key indicators for assessing post-depositional alteration. In the present study, we observe no significant correlations between $\delta^{15}N$ and TOC (Figs. S2d), TN (Figs. S2e), C/N (Figs. S2f), or $\delta^{13}C_{org}$ (Figs. S2g). This demonstrates the $\delta^{15}N$ values retain primary depositional signals without diagenetic or metamorphic overprinting (Kipp et al., 2018; Mettam et al., 2019).

Regarding terrigenous influences, lacustrine systems with substantial terrigenous inputs typically exhibit $\delta^{15}N$ values significantly lower than autochthonous algal organic matter (+5‰ to +10‰), as terrigenous organic materials (e.g., plant debris, soil humus) generally show lower $\delta^{15}N$ values (-2‰ to +5‰) (Talbot, 2002; Shen et al., 2006). While a $\delta^{15}N_{org}$-C/N correlation typically indicates terrestrial influence, its absence in our dataset (Figs. S2f) confirms the $\delta^{15}N_{org}$ values are unaffected by terrigenous input.

5.2 Early Miocene positive carbon isotope excursion and methane release

The pronounced positive carbonate carbon isotope excursion recorded in the Dingqinghu Formation is fundamentally controlled by the fractionation mechanisms of lacustrine carbonate carbon isotopes. Consequently, investigating these fractionation processes not only elucidates the drivers of extreme $\delta^{13}C_{carb}$ excursions but also provide critical insights into the paleolake's carbon cycle dynamics and ecosystem function during this interval. Positive $\delta^{13}C_{carb}$ excursions in lacustrine systems primarily arise from isotope fractionation during three key processes: 1) Enhanced organic matter

https://doi.org/10.5194/egusphere-2025-5342
Preprint. Discussion started: 27 November 2025

296 production and burial, 2) Methane generation and release, and 3) Evaporative CO_2,
297 degassing in saline lakes (Michener and Lajtha, 2008; Thottathil et al., 2022). This
298 study will systematically evaluate these mechanisms to determine their relative
299 contributions to the observed $\delta^{13}C_{carb}$ excursions.

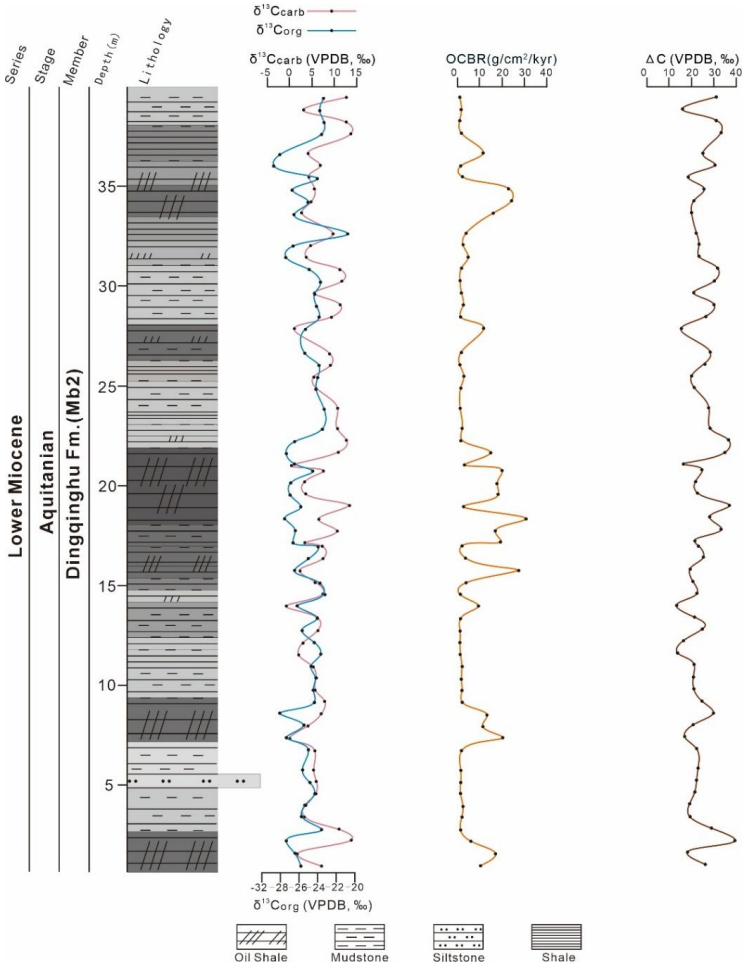

300

301 Figure 3: $\delta^{13}C_{carb}$ (Carbonate carbon isotope), $\delta^{13}C_{org}$ (Organic Carbon Isotope), OCBR (Organic
302 carbon burial rate) and $\Delta^{13}C$ value curses of Dingqinghu Formation.

303 5.2.1 Enhanced organic carbon burial

304 In high-productivity lacustrine systems, variations in carbonate $\delta^{13}C$ values are
305 predominantly controlled by lacustrine productivity (Teranes and McKenzie,

https://doi.org/10.5194/egusphere-2025-5342
Preprint. Discussion started: 27 November 2025

1999;Teranes and Bernasconi, 2005; Zhu, 2013). This relationship arises from photosynthetic fractionation because aquatic plants preferentially assimilate ^{12}C when utilizing CO_2 and bicarbonate from dissolved inorganic carbon (DIC) pools. This process enriches residual DIC ^{13}C, leading to subsequent ^{13}C enrichment in precipitated carbonates (Schelske and Hodell, 1991; Neumann et al., 2002). Under high productivity where aquatic plants preferentially consume dissolved CO_2, the substantial $\delta^{13}C$ difference between bicarbonate (relatively ^{13}C-enriched) and aqueous CO_2 (relatively ^{13}C-depleted) further elevates $\delta^{13}C$ values in both DIC and organic matter (Meyers, 1997; Hodell and Schelske, 1998; Leng and Marshall, 2004; Xu et al, 2006; Zhu et al., 2011). During lake eutrophication, algal blooms generate substantial organic matter while preferentially incorporating ^{12}C. Resultant water column anoxia preserves algal biomass from decomposition, while high sedimentation rates enhance organic carbon burial. Carbonate minerals forming in these ^{12}C-depleted waters consequently exhibit elevated $\delta^{13}C$ values because sequestered ^{12}C remains buried rather than returning to the water column (Müller and Suess, 1979; Calvert, 1987; Ingall et al., 1990; Tyson, 2001; Xu et al., 2004; Wang et al.,2015; Cartapanis et al., 2016; Megan et al.,2021; Wang et al., 2022; Tegler et al., 2024). For the Dingqinghu Formation, the W(V)/W(V+Ni) ratio (Fig. 4) indicates deposition under anoxic/reducing conditions. Corresponding sedimentary facies represent semi-deep and deep lacustrine environments with weak hydrodynamic conditions conducive to sediment preservation. This depositional setting therefore favored efficient organic accumulation and preservation.

Enhanced lacustrine productivity consistently drives both increased carbonate content and elevated $\delta^{13}C$ values in organic matter (Meyers, 1997; Teranes and McKenzie, 1999; Neumann et al., 2002; Leng and Marshall, 2004; Teranes and Bernasconi, 2005; Xu et al., 2006; Lu et al., 2010). C/N values below 10 across most stratigraphic intervals (Fig. 2) indicate autochthonous productivity dominated by aquatic phytoplankton and algae, with negligible terrestrial input. This confirms TOC

https://doi.org/10.5194/egusphere-2025-5342
Preprint. Discussion started: 27 November 2025

serves as a reliable proxy for lacustrine productivity under limited external influences (Meyers, 1997; Zhu et al., 2013). Critically, intervals displaying positive $\delta^{13}C_{carb}$ excursions exhibit extremely low TOC content (average < 1%), indicating depressed productivity. This inverse relationship demonstrates lacustrine productivity cannot explain the observed $\delta^{13}C_{carb}$ excursions. Further supporting this interpretation, high-productivity systems typically yield elevated $\delta^{15}N$ values through two mechanisms. Phytoplankton preferentially assimilate ^{14}N, enriching dissolved inorganic nitrogen pools in ^{15}N. Enhanced denitrification under anoxic conditions further amplifies $\delta^{15}N$ increase in residual nitrogen (Sigman D, 2009). Our data reveal an inverse pattern where positive $\delta^{13}C_{carb}$ excursions systematically coincide with negative $\delta^{15}N$ shift (Fig. 2), demonstrating that the positive $\delta^{13}C_{carb}$ excursion was not caused by enhanced productivity.

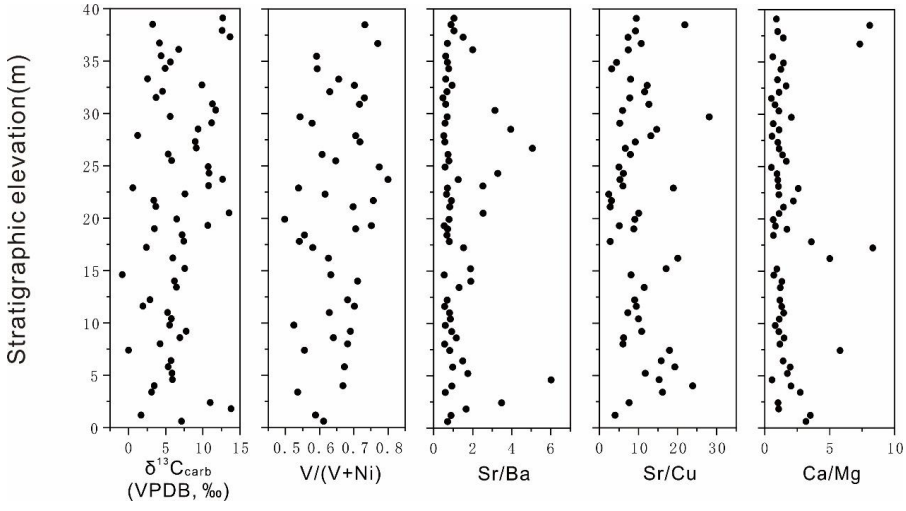

Figure 4: $\delta^{13}C_{carb}$ (Carbonate carbon isotope), V/(V+Ni), Sr/Cu, Sr/Ba and Ca/Mg data in Dingqinghu Formation of lunpola basin.

U-Pb dating and stratigraphic thickness measurements from the Lunpori section indicate a sedimentation rate (SR) of ~107 m/Ma for the study interval of the Dingqinghu Formation (Mao et al., 2019; Xie et al., 2025). The organic carbon burial rate (OCBR) was calculated using the Eq. (1) (Shen et al., 2015):

https://doi.org/10.5194/egusphere-2025-5342
Preprint. Discussion started: 27 November 2025

$$OCBR\ (mg/cm^2/kyr) = SR\ (m/Myr) \times TOC\ (\%) \times \rho\ (g/cm^3), \quad (1)$$

Assuming a bulk rock density (ρ) of 2.5g/cm³, OCBR values for the Dingqinghu Formation in the Lunpori section were derived through unit conversion (summarized in S Table 2). Fig. 3 reveals asynchronous trends between OCBR and the positive $\delta^{13}C_{carb}$ excursion coupled with extremely low correlation coefficient. This strongly suggests that variations in organic carbon burial rate were not the primary driver of the $\delta^{13}C_{carb}$ enrichment observed in the Dingqinghu Formation during this interval.

5.2.2 Evaporation

Strong evaporation in lakes can drive extreme positive carbonate carbon isotope values. This process promotes lake degassing, releasing CO_2 enriched in ^{12}C into the atmosphere. The preferential loss of ^{12}C depletes the DIC pool in light carbon, thereby increasing $\delta^{13}C_{carb}$ (Li and Ku, 1997; Lamb et al., 2007; Zhu et al., 2013; Boscolo-Galazzo et al.,2021). This mechanism is further supported by studies linking evaporative salinity increase to reduced CO_2 solubility and kinetic isotope fractionation during CO_2 efflux (Stiller, 1985). Consequently, arid climates with intense evaporation typically elevate lake salinity and lower lake levels. Palynological data from the Dingqinghu Formation (Xie et al., 2025) reveal alternating dry (e.g., 21.3 Ma, 19.6 Ma) and humid phases (e.g., 20.4 Ma, 20.1 Ma) between 21.4 Ma and 19.4 Ma. At 20.6 Ma, pollen assemblages (Picea, 50.1%; Pinus, 22.2%; Abies, 4.9%; and Fagaceae, 5.2%) indicate warm-humid conditions, consistent with magnetostratigraphic cyclostratigraphic evidence of dry-to-wet cycles (Su et al., 2022). Sr/Cu ratios (Fig. 4) independently confirm warm-arid to warm-humid cyclicity during deposition of the Dingqinghu Formation. Crucially, humid phases reduce evaporation, limiting the ^{12}C-enriched CO_2, and thus diminishing ^{13}C enrichment in the DIC pool. In closed basins like the Lunpola paleolake, evaporation intensity correlates strongly with salinity (Mor et al., 2018; Han et al., 2022), making Ca/Mg ratios an effective salinity proxy (McCormack et al., 2019; Gravina et al., 2022). However, correlation an

https://doi.org/10.5194/egusphere-2025-5342
Preprint. Discussion started: 27 November 2025

alyses of Ca/Mg and Sr/Ba versus $\delta^{13}C_{carb}$ show no significant relationship between salinity changes and $\delta^{13}C_{carb}$ excursion during the Dingqinghu Formation deposition. This lack of correlation demonstrates that salinity variations did not primarily control $\delta^{13}C_{carb}$ trend. Integrated assessment of climate proxies, salinity indicators, and carbon isotopes indicate that while evaporation may contribute secondarily to $\delta^{13}C_{carb}$ enrichment, it was not the principal driver of the observed positive excursion.

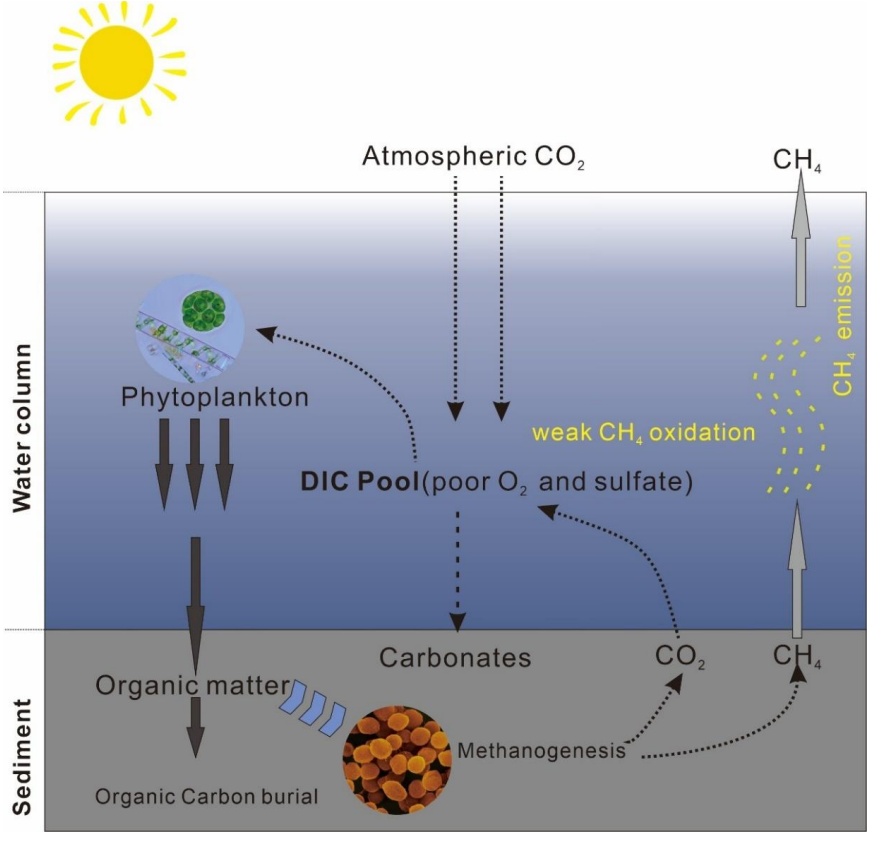

Figure 5: Schematic diagram of the carbon cycling pathway for methane release in Dingqing Lake. Biogenic methane is generated by methanogens in the anoxic sediments, and the water column is under reducing conditions, lacking electron acceptors such as sulfate and iron ions. The methane directly discharges into the atmosphere.

https://doi.org/10.5194/egusphere-2025-5342
Preprint. Discussion started: 27 November 2025

5.2.3 Methane release as the driver of Early Miocene positive $\delta^{13}C_{carb}$ excursion

Methane generation produces significant quantities of CH_4 highly enriched in ^{12}C alongside CO_2 enriched in ^{13}C. The subsequent escape of ^{12}C-enriched CH_4 and the incorporation of ^{13}C-enriched CO_2 into the DIC pool drive $\delta^{13}C_{carb}$ enrichment in DIC-derived carbonates. Based on integrated geochemical evidence, the extreme positive excursion of $\delta^{13}C_{carb}$ in the Dingqinghu Formation likely resulted from substantial kinetic isotope fractionation during methanogenesis. This process facilitated the preferential removal of ^{12}C as CH_4, leaving the DIC pool enriched in $\delta^{13}C_{carb}$. Similar mechanisms are documented in organic-rich lacustrine systems. Examples include Tilo and Lake Bosumtwi, where methanogenesis elevated carbonate $\delta^{13}C$ values to approximately +12‰ (Talbot and Kelts, 1986; Lamb et al., 2007; Rosqvist et al., 2007). Methanogenesis in Lake Apopka generated pore water $\delta^{13}C$ values up to +26.4‰ (Gu et al., 2004), while Lake Dziani Dzaha recorded average carbonate $\delta^{13}C$ values of +16.2 ±1.1‰ (Cadeau et al.,2020). In Lake Caohai, it increased lacustrine carbonate $\delta^{13}C$ to +20.94‰ (Zhu et al.,2013).

Unlike marine sediments dominated by CO_2-reducing methanogenesis (Eq. (R1)), the organic-rich, reducing Lunpola paleolake during Dingqinghu Formation deposition provided an optimal environment for bacterial fermentation. Here acetoclastic methanogenesis (Eq. (R2)) prevailed as the primary methane production pathway (whitticar et al., 1986). Critically, methane fate diverges significantly between marine and lacustrine systems. In marine setting, methane is largely consumed at the Sulfate-Methane Transition Zone (SMTZ) via syntrophy between sulfate-reducing bacteria and anaerobic methanotrophic archaea, with additional aerobic oxidation minimozing atmospheric release (Boetius et al., 2000; Deutzmann and Schink,2011; Mostovaya et al., 2022). Conversely, thinner oxic layers in lakes permit substantial methane bypass of oxidation, leading to significant atmospheric emissions (Sun,2024).

$$CO_2+4H_2 \rightarrow CH_4+2H_2O, \quad \text{(R1)}$$

$$CH_3COOH \rightarrow CH_4+CO_2, \quad \text{(R2)}$$

https://doi.org/10.5194/egusphere-2025-5342
Preprint. Discussion started: 27 November 2025

The carbon isotope fractionation between carbonate and organic matter ($\Delta^{13}C=\delta^{13}C_{carb}$ - $\delta^{13}C_{org}$) serves as a valuable proxy for assessing microbial contributions to sedimentary organic carbon. As established in prior studies (Hayes et al., 1999; Teranes and Bernasconi, 2005; Zhu et al., 2013), $\Delta^{13}C$ approximates εTOC, the isotopic fractionation factor during organic matter synthesis. Significantly, εTOC value >32‰ indicates a dominant bacterial contribution to sedimentary organic matter, while values between 28‰ and 32‰ suggest a mixed phytoplankton-bacterial source (Hayes et al., 1999; Teranes and Bernasconi, 2005; Zhu et al., 2013). Analysis of the Dingqinghu Formation reveals that intervals characterized by enriched δC_{carb} values predominantly exhibit $\Delta^{13}C$ values exceeding 32‰ (Fig. 3). This pronounced fractionation strongly implicates bacterial fermentation and decomposition as the primary processes driving carbon isotope dynamics during these stages. Concurrently depleted TOC values align with the expected signature of intense bacterial organic matter remineralization, further supporting the inference of methane release associated with these microbial processes.

5.3 Lacustrine methane emissions response to Early Miocene warming

The Early Miocene was a pivotal period for climatic change in Asia, primarily driven by the extensive uplift of the Tibetan Plateau and the retreat of the Paratethys Ocean. These processes intensified the Asian monsoon system (Ramstein et al., 1997; Liu and Yin, 2002; Zhang et al., 2007; Boos & Kuang, 2010; Clift & Webb, 2019; Spicer et al., 2021), altering atmospheric circulation and thermal gradients, which in turn led to significant climatic differentiation across the Tibetan Plateau and adjacent areas. The plateau itself is influenced by both the Indian monsoon and continental monsoon systems, resulting in a range of climate regimes from warm and humid to dry and cold (Kutzbach et al., 1993; Guo et al., 2008; Shukla et al., 2014).

Studies by Deng et al. (2019) indicate that during the Miocene, the Indian monsoon dominated the Lunpola Basin, supplying ample moisture and warmth to the region. This interpretation is supported by the presence of subtropical fish fossils in the stratigraphic

https://doi.org/10.5194/egusphere-2025-5342
Preprint. Discussion started: 27 November 2025

record, along with previously documented mammalian fossils, pollen, and spores (Deng et al., 2012; Sun et al., 2014; Jia et al., 2015; Jiang et al., 2018). The monsoon-driven warm and humid conditions fostered high productivity of organic matter within the lake ecosystem, while also promoting the decomposition of organic material by methanogens, leading to substantial methane production (Deng et al., 2019; Su et al., 2019).

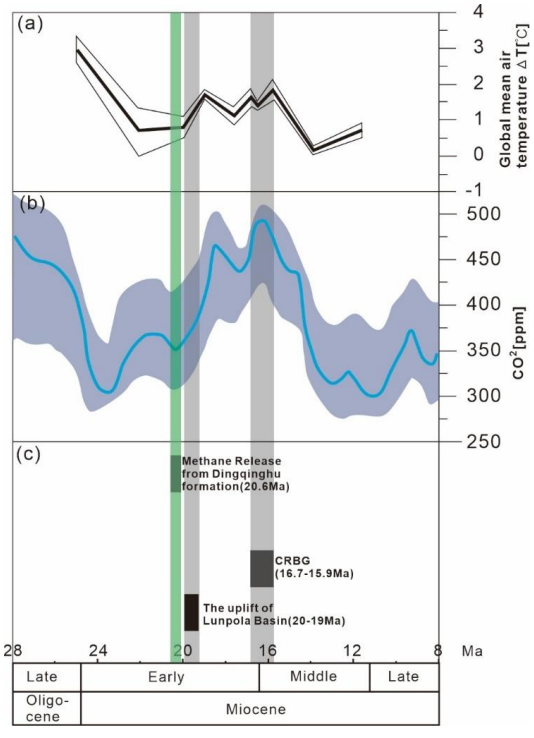

Figure 6:(a)The difference between the global average temperature and today's temperature simulation(Kürschner et al.,2008)； (b) Atmospheric CO2 estimates (symbols) and 500-kyr mean statistical reconstructions (95% credible intervals in dark-blue shading, respectively) (Cenozoic CO2 Proxy Integration Project (CenCO_2PIP) Consortium,2023)； (c) Main geological events of the Miocene, From right to left in order: 1) Methane release from Dingqinghu formation (this study) 2) The uplift of Lunpola basin (Li et al.,2024) 3) CRBG: Columbia River Basalt Group, the largest terrestrial volcanic event in North America(Kasbohm et al.,2018).

Geochemical records from the Dingqinghu Formation in the Lunpola Basin reveal

https://doi.org/10.5194/egusphere-2025-5342
Preprint. Discussion started: 27 November 2025

severely deficient sulfur content (as indicated by whole-rock S data; see Table S2) along with exceptionally low pyrite abundance, suggesting that sulfate concentrations in the paleo-lake were minimal during deposition. This sulfate-limited environment likely suppressed sulfate-driven anaerobic oxidation of methane (SD-AOM). In addition, a reduced oxidation zone further decreased CH_4 consumption, resulting in significant methane efflux into the atmosphere (Fig. 5; Taylor and Macquaker, 2011; Rickard, 2021; Lin et al., 2023).

As a potent greenhouse gas, with a global warming potential 28–34 times that of CO_2 over a 100-year period, methane release from lakes could have contributed substantially to global warming (Forster et al., 2008; Sun et al., 2020). The only known Large Igneous Province (LIP) eruption during the Miocene was the Columbia River Basalt Group, which occurred between approximately 16.7 and 15.9 Ma. This event significantly increased global temperatures and atmospheric CO_2 levels (Fig. 6c; Kasbohm et al., 2018). However, according to Li et al. (2024), major uplift of the Lunpola Basin occurred between 20 and 19 Ma, after the methane release event recorded in the Dingqinghu Formation. This temporal discordance indicates that methane release was not triggered by tectonic uplift (Fig. 6). Furthermore, no contemporary volcanic activity was associated with this methane emission, suggesting that climatic and lacustrine thermal conditions were the primary controls.

Global temperature reconstructions for the Early Miocene indicate a warming trend, accompanied by methane release and rising atmospheric CO_2 levels, which suggests a methane-driven warming event (Fig. 6; Kürschner et al., 2008). In the absence of large igneous province volcanism, this increase in CO_2 can likely attributed to two main processes: (1) the atmospheric oxidation of methane released from the lacustrine deposits, such as those of the Dingqinghu Formation identified in the present study, and (2) additional CO_2 emissions from climate feedback mechanisms amplified by the initial greenhouse warming (Fig. 6; Cenozoic CO_2 Proxy Integration Project ($CenCO_2PIP$) Consortium, 2023). Consequently, methane release from the Tibetan

https://doi.org/10.5194/egusphere-2025-5342
Preprint. Discussion started: 27 November 2025

Plateau may have played an important role in Early Miocene global warming and the concurrent rise in atmospheric CO_2 levels.

As discussed in the preceding sections, a positive feedback mechanism exists between methane release in the Dingqinghu Formation and global climate warming during the Miocene. As temperature rose, lake stratification and anoxia intensified, stimulating microbial methanogenesis and methane ebullition. This released methane was subsequently oxidized to CO_2, further amplifying the greenhouse effect and reinforcing the warming cycle. The Dingqinghu Formation represents a deep-water, anoxic, organic-rich, and semi-restricted lacustrine system with limited external DIC input. To quantify methane ebullition during intervals of pronounced positive carbon isotope excursions in lacustrine sediments, we applied a closed-system Rayleigh fractionation model (Eq. (2)). This method enables estimation of methane emission rates and evaluation of their contribution to atmospheric CO_2, offering direct numerical support for the proposed positive feedback mechanism.

The Rayleigh distillation equation is expressed as (Höhener and Atteia, 2014; Miller et al.,2018; Li et al, 2024):

$$\delta^{13}C_{carb} = \delta^{13}C_{initial} + \varepsilon \cdot ln(f), \quad (2)$$

where $\delta^{13}C_{carb}$ is the measured carbonate carbon isotope composition (% VPDB), $\delta^{13}C_{initial}$ is the initial dissolved inorganic carbon isotope composition (+2%, typical lacustrine background) (Lengs and Marshall, 2004); ε is the fractionation factor (-20% for acetoclastic methanogenesis) (Penning et al., 2006; Valentine et al.,2004; Meister et al.,2019); and f is the fraction of residual DlC.

The fraction of methane lost from the system is then:

$$1 - f = 1 - exp\left(\frac{\delta^{13}C_{carb}+2}{-20}\right), \quad (3)$$

Methane ebullition flux (g CH_4 m^{-2} kyr^{-1}) is calculated as:

$$F_{CH_4} = (1 - f) \times OCBR \times \frac{16}{12}, \quad (4)$$

where OCBR is the measured organic carbon burial rate (g C cm^{-2} kyr^{-1}). Fluxes are converted to g CH_4 m^{-2} yr^{-1} by division by 1000. The full 62-sample dataset with CH4

https://doi.org/10.5194/egusphere-2025-5342
Preprint. Discussion started: 27 November 2025

flux is provided in Supplementary Table S4.

Our calculations show that the paleo-Dingqinghu Lake maintained an average methane flux of 34.5 g CH_4 m^{-2} yr^{-1} (peaking at 151.2 g CH_4 m^{-2} yr^{-1}). After accounting for 30–50% methane loss during atmospheric escape and oxidation, these ebullition events contributed an estimated 3.9–6.6 ppm of atmospheric CO_2 throughout the studied depositional interval. These values provide quantitative evidence that Miocene global warming enhanced lake stratification and anoxia, accelerating organic matter decomposition and methane release. The subsequent oxidation of this methane supplied additional CO_2 to the atmosphere, further strengthening greenhouse conditions and closing a powerful feedback loop. Therefore, paleo-Dingqinghu Lake serves as a clear example of how continental lacustrine systems on the Tibetan Plateau acted as significant amplifiers of global warming during past greenhouse climates, even though their role had been previously underestimated.

6 Conclusions

Our finds establish that the pronounced positive carbonate carbon isotope excursion ($\delta^{13}C_{carb}$ up to +13.79‰) recorded in the Dingqinghu Formation, Lunpola Basin, originated primarily from large-scale methanogenesis and subsequent methane release. Favorable paleoclimate and tectonic conditions promoted organic matter accumulation and methanogenesis, while low sulfate concentrations limited anaerobic methane oxidation, facilitating substantial methane escape to the atmosphere. The observed coupling between this methane release and Early Miocene global atmospheric pCO_2 and temperature rises implicates that Tibetan Plateau methane emissions as a potentially important contributor to in Early Miocene global warming and the coeval increase in atmospheric C

Data availability

All raw data can be provided by the corresponding authors upon request.

https://doi.org/10.5194/egusphere-2025-5342
Preprint. Discussion started: 27 November 2025

Author contributions

CY, XF, and HW: study design, data production, analysis, data interpretation, writing. CY, JD, YW, and TW: sample handling. CY: stable isotope and organic carbon content experiment. CY, XF, and SZ: calculation of methane flux.

Competing interests

The contact author has declared that none of the authors has any competing interests.

Acknowledgements

We thank Ahmed Mansour for providing comprehensive and valuable suggestions.

Financial support

This research was supported funding from the National Natural Science Foundation of China (grant numbers 42241203,42241202, w2433105) and Science and Technology Cooperation Project of the CNPC-SWPU Innovation Alliance (2020Cx0101).

Reference

Altabet, M. A.: Variations in nitrogen isotopic composition between sinking and suspended particles: Implications for nitrogen cycling and particle transformation in the open ocean, Deep-Sea Res. Part I-Oceanogr. Res. Pap., 35: 535-554, https://doi.org/10.1016/0198-0149(88)90130-6, 1988.

Altabet, M. A.: Isotopic tracers of the marine nitrogen cycle: present and past,in: Marine organic matter: biomarkers, isotopes and DNA, edited by: Volkman, J.K., Springer, Berlin, Heidelberg, 251-293, https://doi.org/10.1007/698_2_008, 2006

Bastviken, D., Cole, J., Pace, M., and Tranvik, L.: Methane emissions from lakes: Dependence of lake characteristics, two regional assessments, and a globa

https://doi.org/10.5194/egusphere-2025-5342
Preprint. Discussion started: 27 November 2025

l estimate, Glob. Biogeochem. Cycle., 18, GB4009, https://doi.org/10.1029/2004GB002238, 2004.

Boetius, A., Ravenschlag, K., Schubert, C. J., Rickert, D., Widdel, F., Gieseke, A., Amann, R., Jørgensen, B. B., Witte, U., and Pfannkuche, O.: A marine microbial consortium apparently mediating anaerobic oxidation of methane, Nature, 407, 623-626, https://doi.org/10.1038/35036572, 2000.

Boos, W. R. and Kuang, Z.: Dominant control of the South Asian monsoon by orographic insulation versus plateau heating, Nature, 463: 218-222, https://doi.org/10.1038/nature08707, 2010.

Boscolo-Galazzo, F., Crichton, K. A., Ridgwell, A., Mawbey, E. M., Wade, B. S., and Pearson, P. N.: Temperature controls carbon cycling and biological evolution in the ocean twilight zone. Science, 371, 1148-1152, https://doi.org/10.1126/science.abb6643, 2021.

Cadeau, P., Jézéquel, D., Leboulanger, C., Fouilland, E., Le Floc'h, E., Chaduteau, C., Milesi, V., Guélard, J., Sarazin, G., Katz, A., d'Amore, S., Bernard, C., and Ader, M.: Carbon isotope evidence for large methane emissions to the proterozoic atmosphere, Sci Rep., 10, 18186, https://doi.org/10.1038/s41598-020-75100-x, 2020.

Calvert, S. E.: Oceanographic controls on the accumulation of organic matter in marine sediments, Geol. Soc. London. Spec. Publ., 26, 137–151, https://doi.org/10.1144/GSL.SP.1987.026.01.08, 1987.

https://doi.org/10.5194/egusphere-2025-5342
Preprint. Discussion started: 27 November 2025

590 Cartapanis, O., Bianchi, D., Jaccard, S. L., and Galbraith, E. D.: Global pulses
591 of organic carbon burial in deep-sea sediments during glacial maxima, Nat.
592 Commun., 7, 10796, https://doi.org/10.1038/ncomms10796, 2016.
593 Cenozoic CO_2 Proxy Integration Project (CenCO_2PIP) Consortium: Toward a C
594 enozoic history of atmospheric CO_2, Science, 382, eadi5177, https://doi.org/1
595 0.1126/science.adi5177, 2023.
596 Clift, P. D. and Webb, A. A. G.: A history of the Asian monsoon and its inte
597 ractions with solid Earth tectonics in Cenozoic South Asia, Geol. Soc. Spec.
598 Publ., 483, 631-652, https://doi.org/10.1144/SP483.1, 2019.
599 De Boever, E., Brasier, A. T., Foubert, A., and Kele, S.: What do we really k
600 now about early diagenesis of non-marine carbonates? Sediment. Geol., 361,
601 25–51, https://doi.org/10.1016/j.sedgeo.2017.09.011,2017.
602 Dean, J. F., Middelburg, J. J., Röckmann, T., Aerts, R., Blauw, L. G., Egger,
603 M., Jetten, M. S. M., de Jong, A. E. E., Meisel, O. H., Rasigraf, O., Slomp,
604 C. P., In'T Zandt, M. H., and Dolman, A. J.: Methane feedbacks to the glo
605 bal climate system in a warmer world, Rev. Geophys., 56, 207-250, https://d
606 oi.org/10.1002/2017RG000559, 2018.
607 DelSontro, T., Boutet, L., St-Pierre, A., Del Giorgio, P. A., and Prairie, Y. T.:
608 Methane ebullition and diffusion from northern ponds and lakes regulated by
609 the interaction between temperature and system productivity, Limnol. Oceano
610 gr., 61: S62-S77, https://doi.org/10.1002/lno.10335, 2016.

https://doi.org/10.5194/egusphere-2025-5342
Preprint. Discussion started: 27 November 2025

611 Deng, T., Wang, S., Xie, G., Li, Q., Hou, S., and Sun, B.: A mammalian fossi
612 l from the Dingqing Formation in the Lunpola Basin, northern Tibet, and its
613 relevance to age and paleo-altimetry, Chin. Sci. Bull., 57, 261-269, https://do
614 i.org/10.1007/s11434-011-4773-8, 2012.
615 Deng, T., Wang, X., Wu, F., Wang, Y., Li, Q., Wang, S., and Hou, S.: Implica
616 tions of vertebrate fossils for paleo-elevations of the Tibetan Plateau, Glob.
617 Planet. Change, 174, 58-69, https://doi.org/10.1016/j.gloplacha.2019.01.005, 20
618 19.
619 Deutzmann, J. S., and Schink, B.: Anaerobic oxidation of methane in sediment
620 s of Lake Constance, an oligotrophic freshwater lake, Appl. Environ. Microbi
621 ol., 77, 4429-4436, https://doi.org/10.1128/AEM.00340-11, 2011.
622 Encinas Fernández, J., Peeters, F., and Hofmann, H.: Importance of the autumn
623 overturn and anoxic conditions in the hypolimnion for the annual methane
624 emissions from a temperate lake, Environ. Sci. Technol., 48, 7297-7304, http:
625 //doi.org/10.1021/es4056164, 2014.
626 Fang, X., Dupont-Nivet, G., Wang, C., Song, C., Meng, Q., Zhang, W., Nie, J.,
627 Zhang, T., Mao, Z., and Chen, Y.: Revised chronology of central Tibet upli
628 ft (Lunpola Basin), Sci. Adv., 6, eaba7298, http://doi.org/10.1126/sciadv.aba72
629 98, 2020.
630 Forster, P., Ramaswamy, V., Artaxo, P., Berntsen, T., Betts, R., Fahey, D., Hay
631 wood, J., Lean, J., Lowe, D., Myhre, G., Nganga, J., Prinn, R., Raga, G., S

https://doi.org/10.5194/egusphere-2025-5342
Preprint. Discussion started: 27 November 2025

chulz, M., and Van Dorland, R.: Changes in atmospheric constituents and in radiative forcing, in: Climate Change 2007: The Physical Science Basis, edited by: Solomon, S., Qin, D., Manning, M., Marquis, M., Averyet, K., and Melinda M. B., Cambridge University Press, Cambridge, UK, 129–134, ISBN 9780521705967, 2008.

Freudenthal, T., Wagner, T., Wenzhöfer, F., Zabel, M., and Wefer, G.: Early diagenesis of organic matter from sediments of the eastern subtropical Atlantic: evidence from stable nitrogen and carbon isotopes, Geochim. Cosmochim. Acta, 65, 1795-1808, https://doi.org/10.1016/S0016-7037(01)00554-3, 2001.

Fu, X., Wang, J., Tan, F., Feng, X., Wang, D., and Song, C.: Geochemistry of terrestrial oil shale from the Lunpola area, northern Tibet, China, Int. J. Coal Geol., 102, 1–11, https://doi.org/10.1016/j.coal.2012.08.005, 2012.

Fu, X., Wang, J., Chen, W., Feng, X., Wang, D., Song, C., and Zeng, S.: Organic accumulation in lacustrine rift basin: constraints from mineralogical and multiple geochemical proxies, Int. J. Earth Sci., 104, 495–511, https://doi.org/10.1007/s00531-014-1089-3, 2015.

Fu, X., Wang, J., Wen, H., Wang, Z., Zeng, S., Song, C., Wang, D., and Nie, Y.: Carbon-isotope record and paleoceanographic changes prior to the OAE 1a in the Eastern Tethys: Implication for the accumulation of organic-rich sediments, Mar. Pet. Geol., 113, 104049, https://doi.org/10.1016/j.marpetgeo.2019.104049, 2020.

https://doi.org/10.5194/egusphere-2025-5342
Preprint. Discussion started: 27 November 2025

653 Gravina, P., Ludovisi, A., Moroni, B., Vivani, R., Selvaggi, R., Petroselli, C., a
654 nd Cappelletti, D.: Geochemical proxies and mineralogical fingerprints of sed
655 imentary processes in a closed shallow lake basin since 1850, Aquat. Geoche
656 m., 28, 43-62, https://doi.org/10.1007/s10498-022-09403-y, 2022.
657 Gu, B., Schelske, C. L., and Hodell, D. A.: Extreme 13c enrichments in a sha
658 llow hypereutrophic lake: implications for carbon cycling, Limnol. Oceanogr.,
659 49, 1152-1159, **https://doi.org/10.4319/lo.2004.49.4.1152**, 2004.
660 Guo, Z., Sun, B., Zhang, Z., Peng, S., Xiao, G., Ge, J., Hao, Q., Qiao, Y., Li
661 ang, M., Liu, J., Yin, Q., and Wei, J.: A major reorganization of Asian clim
662 ate by the early Miocene, Clim. Past, 4, 153–174, https://doi.org/10.5194/cp-4
663 -153-2008, 2008.
664 Gutjahr, M., Ridgwell, A., Sexton, P. F., Anagnostou, E., Pearson, P. N., Pälik
665 e, H., Norris, R. D., Thomas, E., and Foster, G. L.: Very large release of m
666 ostly volcanic carbon during the Palaeocene–Eocene Thermal Maximum, Natu
667 re, 548, 573-577, https://doi.org/10.1038/nature23646, 2017.
668 Han, L., Li, Y., Zou, Y., Gao, X., Gu, Y., and Wang, L.: Relationship between
669 lake salinity and the climatic gradient in northeastern China and its implicat
670 ions for studying climate change, Sci. Total Environ., 805: 150403, https://do
671 i.org/10.1016/j.scitotenv.2021.150403, 2022.
672 Hayes, J. M., Strauss, H., and Kaufman, A. J.: The abundance of 13C in mari
673 ne organic matter and isotopic fractionation in the global biogeochemical cyc

https://doi.org/10.5194/egusphere-2025-5342
Preprint. Discussion started: 27 November 2025

674 le of carbonduring the past 800 Ma, Chem. Geol., 161, 103-125, https://doi.o
675 rg/10.1016/S0009-2541(99)00083-2, 1999.
676 Hillaire-Marcel, C., Kim, S., Landais, A., Ghosh, P., Assonov, S., Lécuyer, C.,
677 Blanchard, M., Meijer, H. A. J., and Steen-Larsen, H. C.: A stable isotope t
678 oolbox for water and inorganic carbon cycle studies, Nat. Rev. Earth. Env.,
679 2, 699–719, http://doi.org/10.1038/s43017-021-00209-0, 2021.
680 Hodell, D. A. and Schelske, C. L.: Production, sedimentation, and isotopic com
681 position of organic matter in Lake Ontario, Limnol. Oceanogr., 43, 200-214,
682 https://doi.org/10.4319/lo.1998.43.2.0200, 1998.
683 Höhener, P. and Atteia, O.: Rayleigh equation for evolution of stable isotope ra
684 tios in contaminant decay chains, Geochim. Cosmochim. Acta, 126, 70-77, ht
685 tps://doi.org/10.1016/j.gca.2013.10.036, 2013.
686 Hollander, D. J. and Smith, M. A.: Microbially mediated carbon cycling as a c
687 ontrol on the $\delta^{13}C$ of sedimentary carbon in eutrophic Lake Mendota (USA):
688 new models for interpreting isotopic excursions in the sedimentary record,
689 Geochim. Cosmochim. Acta, 65, 4321-4337, https://doi.org/10.1016/S0016-703
690 7(00)00506-8, 2001.
691 Horacek M., Brandner R., and Abart R.: Carbon isotope record of the P/T bou
692 ndary and the Lower Triassic in the Southern Alps: evidence for rapid chan
693 ges in storage of organic carbon, Paleogeogr. Paleoclimatol. Paleoecol., 252,
694 347–354, https://doi.org/10.1016/j.palaeo.2006.11.049, 2007.

https://doi.org/10.5194/egusphere-2025-5342
Preprint. Discussion started: 27 November 2025

695 Hu, D., Li, D., Zhou, L., Sun, L., and Xu, Y.: Diagenetic effects on strontium
696 isotope (^{87}Sr/^{86}Sr) and elemental (Sr, Mn, and Fe) signatures of Late Ordo
697 vician carbonates, J. Univ. Sci. Technol. China, 53, 0503-1-0503-10, http://do
698 i.org/10.52396/JUSTC-2022-0160, 2023.
699 Huntington K. W. and Petersen S. V.: Frontiers of carbonate clumped isotope t
700 hermometry, Annu. Rev. Earth Planet. Sci., 51, 611-641, https://doi.org/10.114
701 6/annurev-earth-031621-085949, 2023.
702 Ingall, E. D., and Cappellen, P. V.: Relation between sedimentation rate and bu
703 rial of organic phosphorus and organic carbon in marine sediments, Geochim.
704 Cosmochim. Acta, 54, 373–386, https://doi.org/10.1016/0016-7037(90)90326-
705 G, 1990.
706 Ivany, L. C., del Río, C. J., Alvarez, M. J., Acosta, R. P., Lohmann, K. C., a
707 nd Raigemborn, M. S.: Approaching the Miocene Climatic Optimum in Pata
708 gonia (southern Argentina): Temperature seasonality and a potential role for t
709 he opening Drake Passage, Paleoceanogr. Paleoclimatology, 40, e2025PA0051
710 00, https://doi.org/10.1029/2025PA005100, 2025.
711 Kender, S., Bogus, K., Pedersen, G. K., Dybkjær, K., Mather, T. A., Mariani,
712 E., Ridgwell, A., Riding, J. B., Wagner, T., Hesselbo, S. P., and Leng, M. J.:
713 Paleocene/Eocene carbon feedbacks triggered by volcanic activity, Nat. Com
714 mun., 12, 5186, https://doi.org/10.1038/s41467-021-25536-0, 2021.
715 Kipp, M. A., Stüeken, E. E., Yun, M., Bekker, A., and Buick, R.: Pervasive a

https://doi.org/10.5194/egusphere-2025-5342
Preprint. Discussion started: 27 November 2025

716 ero-bic nitrogen cycling in the surface ocean across the Paleopro-terozoic Er
717 a, Earth Planet. Sci. Lett., 500,117-126, https://doi.org/10.1016/j.epsl.2018.08.0
718 07, 2018.
719 Kürschner, W. M., Kvaček, Z., and Dilcher, D. L.: The impact of Miocene at
720 mospheric carbon dioxide fluctuations on climate and the evolution of terrest
721 rial ecosystems, Proc. Natl. Acad. Sci., 105, 449-453, http://doi.org/10.1073/p
722 nas.0708588105, 2008.
723 Lamb, H. F., Leng, M. J., Telford, R. J., Ayenew, T., and Umer, M.: Oxygen
724 and carbon isotope composition of authigenic carbonate from an Ethiopian la
725 ke: a climate record of the last 2000 years, The Holocene, 17, 515-524, http:
726 //doi.org/10.1177/0959683607076452, 2007.
727 Lehmann, M. F., Bernasconi, S. M., Barbieri, A., and Mckenzie, J. A.: Preserv
728 ation of organic matter and alteration of its carbon and nitrogen isotope com
729 position during simulated and in situ early sedimentary diagenesis, Geochim.
730 Cosmochim. Acta, 2002, 3573-3584, https://doi.org/10.1016/S0016-7037(02)009
731 68-7, 2002.
732 Lei Q., Fu X., and Lu Y.: Petroleum geological features of Tertiary terrestrial
733 Lunpola basin, Tibet,in: Geology of Fossil Fuels --- Oil and Gas : Proceedin
734 gs of the 30th International Geological Congress, edited by: Sun, Z.C., Wan
735 g, T.B., Ye, D.L., and Song, G.J., 11, https://doi.org/10.1201/9780429087837,
736 1997.

https://doi.org/10.5194/egusphere-2025-5342
Preprint. Discussion started: 27 November 2025

737 Leng, M. J. and Marshall, J. D.: Palaeoclimate interpretation of stable isotope
738 data from lake sediment archives, Quat. Sci. Rev., 23, 811-831, https://doi.or
739 g/10.1016/j.quascirev.2003.06.012, 2004.
740 Li, L., Garzione, C. N., Lu, H., and Quade, J.: Neogene surface uplift of the
741 Lunpola Basin in Central Tibet: Implications for uplifting and flattening of o
742 rogenic plateaus, Earth Planet. Sci. Lett., 646, 118961, https://doi.org/10.1016/
743 j.epsl.2024.118961, 2024.
744 Li, W., Wang, J., Jia, C., Lu, S., Li, J., Zhang, P., Wei, Y., Song, Z., Chen,
745 G., and Zhou, N.: Carbon isotope fractionation during methane transport thro
746 ugh tight sedimentary rocks: phenomena, mechanisms, characterization, and i
747 mplications, Geosci. Front., 15, 101912, https://doi.org/10.1016/j.gsf.2024.1019
748 12, 2024.
749 Lin, Z., Strauss, H., Peckmann, J., Roberts, A. P., Lu, Y., Sun, X., Chen, T., a
750 nd Harzhauser, M.: Seawater sulphate heritage governed early late miocene
751 methane consumption in the long-lived lake pannon, Commun. Earth Enviro
752 n., 4, 207, https://doi.org/10.1038/s43247-023-00879-2, 2023.
753 Liu, X. and Yin, Z.: Sensitivity of East asian monsoon climate to the uplift of
754 the Tibetan Plateau, Palaeogeogr, Palaeoclimatol. Palaeoecol., 183, 223–245,
755 https://doi.org/10.1016/S0031-0182(01)00488-6, 2002.
756 Liu, Q., Li, P., Jin, Z., Sun, Y., Hu, G., Zhu, D., Huang, Z., Liang, X., Zhan
757 g, R., and Liu, J.: Organic-rich formation and hydrocarbon enrichment of lac

https://doi.org/10.5194/egusphere-2025-5342
Preprint. Discussion started: 27 November 2025

758 ustrine shale strata: A case study of Chang 7 Member, Sci. China Earth Sci.,
759 65, 118-138, https://doi.org/10.1007/s11430-021-9819-y, 2022.
760 Lourey, M. J., Trull, T. W., and Sigman, D. M.: Sensitivity of δ15N of nitrate,
761 surface suspended and deep sinking particulate nitrogen to seasonal nitrate d
762 epletion in the Southern Ocean, Glob. Biogeochem. Cycle., 17, 1081, https://
763 doi.org/10.1029/2002GB001973, 2003.
764 Lu, Y., Meyers, P. A., Eadie, B. J., and Robbins, J. A.: Carbon cycling in Lak
765 e Erie during cultural eutrophication over the last century inferred from the
766 stable carbon isotope composition of sediments, J. Paleolimn., 43, 261-272, h
767 ttps://doi.org/10.1007/s10933-009-9330-y, 2010.
768 Lu, J., Fu, X., Du, Q., Nie, Y., Wei, H., Zhou, G., and Wang, W.: Climate-ind
769 uced organic matter enrichment in lacustrine basin: Insights from the Palaeog
770 ene–Neogene oil shale in the Lunpola Basin (Tibet, China), Geol. J., 2023,
771 58, 4057-4069, https://doi.org/10.1002/gj.4758, 2023.
772 Bižić, M., Klintzsch, T., Ionescu, D., Hindiyeh, M. Y., Günthel, M., Muro-Past
773 or, A. M., Eckert, W., Urich, T., Keppler, F., and Grossart, H. P.: Aquatic a
774 nd terrestrial cyanobacteria produce methane, Sci. Adv., 6, eaax5343, http://d
775 x.doi.org/10.1126/sciadv.aax5343, 2020.
776 Ma, P., Wang, L., Wang, C., Wu, X., and Wei, Y.: Organic-matter accumulatio
777 n of the lacustrine Lunpola oil shale, central Tibetan Plateau: Controlled by
778 the paleoclimate, provenance, and drainage system, Int. J. Coal Geol., 147–1

https://doi.org/10.5194/egusphere-2025-5342
Preprint. Discussion started: 27 November 2025

779 48, 58–70, https://doi.org/10.1016/j.coal.2015.06.011, 2015.
780 Ma, P., Wang, C., Meng, J., Ma, C., Zhao, X., Li, Y., and Wang, M.: Late Ol
781 igocene-early Miocene evolution of the Lunpola Basin, central Tibetan Platea
782 u, evidences from successive lacustrine records, Gondwana Res., 48: 224-236,
783 https://doi.org/10.1016/j.gr.2017.04.023, 2017.
784 Macko, S. A., Fogel, M. L., Hare, P. E., and Hoering, T. C.: Isotopic fractiona
785 tion of nitrogen and carbon in the synthesis of amino acids by microorganis
786 ms, Chemical Geology: Isotope Geoscience section, 65, 79-92, https://doi.org/
787 10.1016/0168-9622(87)90064-9, 1987.
788 Mao, Z., Meng, Q., Fang, X., Zhang, T., Wu, F., Yang, Y., Zhang, W., Zan, J.,
789 and Tan, M.: Recognition of tuffs in the middle-upper dingqinghu fm., Lun
790 pola basin, central tibetan plateau: constraints on stratigraphic age and implic
791 ations for paleoclimate, Paleogeogr. Paleoclimatol. Paleoecol., 525, 44-56, htt
792 ps://doi.org/10.1016/j.palaeo.2019.03.040, 2019.
793 Martens C. S. and Berner R. A.: Methane production in the interstitial waters
794 of sulfate-depleted marine sediments, Science, 185, 1167-1169, http://dx.doi.or
795 g/10.1126/science.185.4157.1167, 1974.
796 McCormack, J., Viehberg, F., Akdemir, D., Immenhauser, A., and Kwiecien, O.:
797 Ostracods as ecological and isotopic indicators of lake water salinity change
798 s: the Lake Van example, Biogeosciences, 16, 2095-2114, https://doi.org/10.51
799 94/bg-16-2095-2019, 2019.

https://doi.org/10.5194/egusphere-2025-5342
Preprint. Discussion started: 27 November 2025

800 Meister, P., Liu, B., Khalili, A., Böttcher, M.E., and Jørgensen, B.B.: Factors c
801 ontrolling the carbon isotope composition of dissolved inorganic carbon and
802 methane in marine porewater: an evaluation by reaction-transport modelling,
803 J. Mar. Syst., 200, 103227, https://doi.org/10.1016/j.jmarsys.2019.103227, 201
804 9.
805 Methner, K., Campani, M., Fiebig, J., Löffler, N., Kempf, O., and Mulch, A.:
806 Middle Miocene long-term continental temperature change in and out of pace
807 with marine climate records, Sci Rep, 10, 7989, https://doi.org/10.1038/s415
808 98-020-64743-5, 2020.
809 Mettam, C., Zerkle, A. L., Claire, M. W., Prave, A. R., Poulton, S. W., and J
810 unium, C. K.: Anaero-bic nitrogen cycling on a Neoarchaean ocean margin,
811 Earth Planet. Sci. Lett., 527, 115800, https://doi.org/10.1016/j.epsl.2019.11580
812 0, 2019.
813 Meyers, P. A.: Organic geochemical proxies of paleoceanographic, paleolimnolo
814 gic, and paleoclimatic processes, Org. Geochem., 27, 213-250, https://doi.org/
815 10.1016/S0146-6380(97)00049-1, 1997.
816 Michener, R., and Lajtha, K. (Eds.): Stable isotopes in ecology and environmen
817 tal science, John Wiley and Sons, 566pp., ISBN 9780470691854, 2008.
818 Miller, H.M., Chaudhry, N., Conrad, M.E., Bill, M., Kopf, S.H., and Templeto
819 n, A.S.: Large carbon isotope variability during methanogenesis under alkalin
820 e conditions, Geochim. Cosmochim. Acta, 237, 18-31, https://doi.org/10.1016/

https://doi.org/10.5194/egusphere-2025-5342
Preprint. Discussion started: 27 November 2025

j.gca.2018.06.007, 2018.

Mor, Z., Assouline, S., Tanny, J., Lensky, I. M., and Lensky, N. G.: Effect of water surface salinity on evaporation: The case of a diluted buoyant plume o ver the Dead Sea, Water Resour. Res., 54, 1460-1475, https://doi.org/10.1002/2017WR021995, 2018.

Mostovaya, A., Wind-Hansen, M., Rousteau, P., Bristow, L. A., and Thamdrup, B.: Sulfate-and iron-dependent anaerobic methane oxidation occurring side-by-side in freshwater lake sediment, Limnol. Oceanogr., 67, 231-246, https://doi.org/10.1002/lno.11988, 2022.

Müller, P. J. and Suess, E.: Productivity, sedimentation rate, and sedimentary or ganic matter in the oceans–I. Organic carbon preservation. Deep-Sea Res. Pa rt I-Oceanogr. Res. Pap., 26, 1347–1362, https://doi.org/10.1016/0198-0149(79)90003-7, 1979.

Neumann, T., Stögbauer, A., Walpersdorf, E., Stüben, D., and Kunzendorf, H.: Stable isotopes in recent sediments of Lake Arendsee, NE Germany: respons e to eutrophication and remediation measures, Paleogeogr. Paleoclimatol. Pale oecol., 178, 75-90, https://doi.org/10.1016/S0031-0182(01)00403-5, 2002.

Nie, Y., Fu, X., Liu, X., Wei, H., Zeng, S., Lin, F., Wan, Y., and Song, C.: O rganic matter accumulation mechanism under global/regional warming: Insight from the Late Barremian calcareous shales in the Qiangtang Basin (Tibet), J. Asian Earth Sci., 241: 105456, https://doi.org/10.1016/j.jseaes.2022.105456,

https://doi.org/10.5194/egusphere-2025-5342
Preprint. Discussion started: 27 November 2025

2023.

Papineau, D., Purohit, R., Goldberg, T., Pi, D., Shields, G. A., Bhu, H., Steele, A., and Fogel, M. L.: High primary productivity and nitrogen cycling after the Paleoproterozoic phosphogenic event in the Aravalli Supergroup, India, Precambrian Res., 171, 37-56, https://doi.org/10.1016/j.precamres.2009.03.005, 2009.

Penning, H., Claus, P., Casper, P., and Conrad, R.: Carbon isotope fractionation during acetoclastic methanogenesis by methanosaeta concilii in culture and a lake sediment, Appl. Environ. Microbiol., 72, 5648-5652, https://doi.org/10.1128/AEM.00727-06, 2006.

Ramstein, G., Fluteau, F., Besse, J., and Joussaume, S.: Effect of orogeny, plate motion and land–sea distribution on Eurasian climate change over the past 30 million years, Nature, 386, 788–795, https://doi.org/10.1038/386788a0, 1997.

Rickard, D. (Eds.): Framboids, Oxford University Press, Oxford Academic, https://doi.org/10.1093/oso/9780190080112.001.0001,2021.

Ritter, A., Mavromatis, V., Dietzel, M., Kwiecien, O., Wiethoff, F., Griesshaber, E., Casella, L. A., Schmahl, W. W., Koelen, J., Neuser, R. D., Leis, A., Buhl, D., Niedermayr, A., Breitenbach, S. F. M., Bernasconi, S. M., and Immenhauser, A.: Exploring the impact of diagenesis on (isotope) geochemical and microstructural alteration features in biogenic aragonite, Sedimentology, 64,

https://doi.org/10.5194/egusphere-2025-5342
Preprint. Discussion started: 27 November 2025

1354-1380, https://doi.org/10.1111/sed.12356, 2017.

Robinson, R. S., Kienast, M., Luiza Albuquerque, A., Altabet, M., Contreras, S., De Pol Holz, R., Dubois, N., Francois, R., Galbraith, E., Hsu, T., Ivanochko, T., Jaccard, S., Kao, S., Kiefer, T., Kienast, S., Lehmann, M., Martinez, P., Mccarthy, M., Möbius, J., Pedersen, T., Quan, T. M., Ryabenko, E., Schmittner, A., Schneider, R., Schneider-Mor, A., Shigemitsu, M., Sinclair, D., Somes, C., Studer, A., Thunell, R., and Yang, J.: A review of nitrogen isotopic alteration in marine sediments, Paleoceanography, 2012, 27, PA4203, https://doi.org/10.1029/2012PA002321, 2012.

Rowley, D. and Currie, B.: Palaeo-altimetry of the late Eocene to Miocene Lunpola basin, central Tibet, Nature, 439, 677-681, https://doi.org/10.1038/nature04506, 2006.

Schelske, C. L. and Hodell, D. A.: Recent changes in productivity and climate of LakeOntario detected by isotopic analysis of sediments, Limnol. Oceanogr., 36, 961-975, https://doi.org/10.4319/lo.1991.36.5.0961, 1991.

Shen, R. F., Cai, H., and Gong, W. H.: Transgenic Bt cotton has no apparent effect on enzymatic activities or functional diversity of microbial communities in rhizosphere soil, Plant Soil, 285, 149-159, https://doi.org/10.1007/s11104-006-9000-z, 2006.

Shukla, A., Mehrotra, R. C., Spicer, R. A., Spicer, T. E. V., and Kumar, M.: Cool equatorial terrestrial temperatures and the South Asian monsoon in the

https://doi.org/10.5194/egusphere-2025-5342
Preprint. Discussion started: 27 November 2025

884 Early Eocene: Evidence from the Gurha Mine, Rajasthan, India, Paleogeogr.
885 Paleoclimatol. Paleoecol., 412, 187–198, https://doi.org/10.1016/j.palaeo.2014.0
886 8.004, 2014.
887 Sigman, D. M., Karsh, K. L., and Casciotti, K. L.: Ocean Process Tracers: Nit
888 rogen Isotopes in the Ocean, in: Encyclopedia of Ocean Sciences, edited by:
889 Steel, J., Thorpe, S., and Turekian, K., Academic Press,4138-4153, https://hdl.
890 handle.net/102.100.100/534313, 2009.
891 Spicer, R. A., Su, T., Valdes, P. J., Farnsworth, A., Wu, F., Shi, G., Spicer, T.
892 E. V., and Zhou, Z.: The topographic evolution of the Tibetan Region as rev
893 ealed by palaeontology, Palaeobiodiversity Palaeoenvironments, 101, 213-243,
894 https://doi.org/10.1007/s12549-020-00452-1, 2021.
895 Su, B., Sun, J., and Jin, C.: Orbital forcing of climatic changes on the central
896 tibetan plateau reveals late oligocene to early miocene south asian monsoon
897 evolution, Geophys. Res. Lett., 49, e2021GL097428, https://doi.org/10.1029/20
898 21GL097428, 2022.
899 Sun, F., Hu, W., Wang, X., Cao, J., Fu, B., Wu, H., and Yang, S.: Methanoge
900 n microfossils and methanogenesis in permian lake deposits, Geology, 49, 13
901 -18, https://doi.org/10.1130/G47857.1, 2020.
902 Sun, F., Hu, W., Cao, J., Wang, X., Zhang, Z., Ramezani, J., and Shen, S.: Su
903 stained and intensified lacustrine methane cycling during Early Permian clima
904 te warming, Nat. Commun., 13, 4856, https://doi.org/10.1038/s41467-022-3243

https://doi.org/10.5194/egusphere-2025-5342
Preprint. Discussion started: 27 November 2025

905 8-2, 2022.

906 Sun, F., Luo, G., Pancost, R. D., Dong, Z., Li, Z., Wang, H., Chen, Z., and
907 Xie, S.: Methane fueled lake pelagic food webs in a cretaceous greenhouse
908 world, Proc. Natl. Acad. Sci., 121, e2411413121, https://doi.org/10.1073/pnas.
909 2411413121, 2024.

910 Talbot, M. R.: Nitrogen isotopes in palaeolimnology, in: Tracking environmental
911 change using lake sediments: physical and geochemical methods, edited by:
912 Last, W.M. and Smol, J.P., Springer, Dordrecht ,2, 401-439, https://doi.org/10.
913 1007/0-306-47670-3_15, 2002.

914 Taylor, K. G. and Macquaker, J. H. S.: Iron minerals in marine sediments reco
915 rd chemical environments, Elements, 7, 113–118, https://doi.org/10.2113/gsele
916 ments.7.2.113, 2011.

917 Tegler, L. A., Horner, T. J., Galy, V. V., Bent, S., Wang, Y., Kim, H. H., Met
918 e, O. Z., and Nielsen, S. G.: Distribution and drivers of organic carbon sedi
919 mentation along the continental margins, AGU Adv., 5, e2023AV001000, http
920 s://doi.org/10.1029/2023AV001000, 2024.

921 Teranes, J. L., Mckenzie, J. A., Lotter, A. F., and Sturm, M.: Stable isotope re
922 sponse to lake eutrophication: calibration of a high-resolution lacustrine seque
923 nce from Baldeggersee, Switzerland, Limnol. Oceanogr., 44, 320-333, https://
924 doi.org/10.4319/lo.1999.44.2.0320, 1999.

925 Teranes, J. L. and Bernasconi, S. M.: Factors controlling $\delta^{13}C$ values of sedim

https://doi.org/10.5194/egusphere-2025-5342
Preprint. Discussion started: 27 November 2025

926 entary carbon in hypertrophic Baldeggersee, Switzerland, and implications for
927 interpreting isotope excursions in lake sedimentary records, Limnol. Oceanog
928 r., 50, 914-922, https://doi.org/10.4319/lo.2005.50.3.0914, 2005.
929 Thottathil, S. D., Reis, P. C. J., and Prairie, Y. T.: Variability and controls of
930 stable carbon isotopic fractionation during aerobic methane oxidation in temp
931 erate lakes, Front. Environ. Sci., 10, 833688, https://doi.org/10.3389/fenvs.202
932 2.833688, 2022.
933 Tremblin, M., Khozyem, H., Adatte, T., Spangenberg, J. E., Fillon, C., Grauls,
934 A., Hunger, T., Nowak, A., Läuchli, C., Lasseur, E., Roig, J., Serrano, O., C
935 alassou, S., Guillocheau, F., and Castelltort, S.: Mercury enrichments of the
936 Pyrenean foreland basins sediments support enhanced volcanism during the P
937 aleocene-Eocene thermal maximum (PETM), Glob. Planet. Change, 212, 1037
938 94, https://doi.org/10.1016/j.gloplacha.2022.103794, 2022.
939 Tyson, R. V.: Sedimentation rate, dilution, preservation and total organic carbon:
940 some results of a modelling study, Org. Geochem., 32, 333–339, https://doi.
941 org/10.1016/S0146-6380(00)00161-3, 2001.
942 Valentine, D.L., Chidthaisong, A., Rice, A., Reeburgh, W.S., and Tyler, S.C.: C
943 arbon and hydrogen isotope fractionation by moderately thermophilic methano
944 gens, Geochim. Cosmochim. Acta, 68, 1571-1590, https://doi.org/10.1016/j.gca.
945 2003.10.012, 2004.
946 Wang, C., Zhao, X., Liu, Z., Lippert, P. C., Graham, S. A., Coe, R. S., Yi, H.,

https://doi.org/10.5194/egusphere-2025-5342
Preprint. Discussion started: 27 November 2025

947 Zhu, L., Liu, S., and Li, Y.: Constraints on the early uplift history of the
948 Tibetan Plateau, Proc. Natl. Acad. Sci., 105, 4987-4992, https://doi.org/10.107
949 3/pnas.0703595105, 2008.
950 Wang, G., Jia, Y., and Li, W.: Effects of environmental and biotic factors on c
951 arbon isotopic fractionation during decomposition of soil organic matter, Sci
952 Rep, 5, 11043, https://doi.org/10.1038/srep11043, 2015.
953 Wang, D., Liu, Y., Zhang, J., Lang, Y., Li, Z., Tong, Z., Xu, L., Su, Z., and
954 Niu, J.: Controls on marine primary productivity variation and organic matter
955 accumulationduring the Late Ordovician-Early Silurian transition, Mar. Pet.
956 Geol., 142, 105742, https://doi.org/10.1016/j.marpetgeo.2022.105742, 2022.
957 Wang, J., Wang, Z., Fu, X., Wang, X., Wilde, S.A., Fu, Y., Lin, J., Wei, H.,
958 Shen, L., Rao, G., and Mansour, A.: Control of stepwise subduction and sla
959 b breakoff on volcanism and uplift in the Tibetan Plateau, Earth Planet. Sci.
960 Lett., 647, 119057, https://doi.org/10.1016/j.epsl.2024.119057, 2024.
961 Wang, L., Li, Y., Shen, L., Han, Z., Peng, H., Li, X., and Wei, Y.: Sedimentar
962 y evolution and hydrocarbon resource potential of Cenozoic continental basin
963 s in the Tibetan Plateau, Acta Petrol. Sin., 41, 1101-1119, https://doi.org/10.1
964 8654/1000-0569/2025.03.20, 2025.
965 Wei, W., Lu, Y., Xing, F., Liu, Z., Pan, L., and Algeo, T. J.: Sedimentary faci
966 es associations and sequence stratigraphy of source and reservoir rocks of th
967 e lacustrine Eocene Niubao Formation (Lunpola Basin, central Tibet), Mar. P

https://doi.org/10.5194/egusphere-2025-5342
Preprint. Discussion started: 27 November 2025

et. Geol., 86, 1273–1290, https://doi.org/10.1016/j.marpetgeo.2017.07.032, 2017.

Whiticar, M. J.: Carbon and hydrogen isotope systematics of bacterial formation and oxidation of methane, Chem. Geol., 161, 291-314, https://doi.org/10.1016/S0009-2541(99)00092-3, 1999.

Wynn, J. G.: Carbon isotope fractionation during decomposition of organic matter in soils and paleosols: Implications for paleoecological interpretations of paleosols, Paleogeogr. Paleoclimatol. Paleoecol., 251, 437-448, https://doi.org/10.1016/j.palaeo.2007.04.009, 2007.

Xia, L., Cao, J., Stüeken, E. E., Hu, W., and Zhi, D.: Linkages between nitrogen cycling, nitrogen isotopes, and environmental properties in paleo-lake basins, Geol. Soc. Am. Bull., 134, 2359-2372, https://doi.org/10.1130/B36290.1, 2022.

Xie, Y., Balázs, A., Gerya, T., and Xiong, X.: Uplift of the Tibetan Plateau driven by mantle delamination from the overriding plate, Nat. Geosci., 17, 683-688, https://doi.org/10.1038/s41561-024-01473-7, 2024.

Xie, G., Li, J., Yao, Y., Wang, S., Sun, B., Ferguson, D. K., Li, C., Li, M., Deng, T., and Wang, Y.: Palynological evidence reveals vegetation succession in the central qinghai-tibet plateau during the late oligocene to early Miocene, J. Syst. Evol., 63, 53-61, https://doi.org/10.1111/jse.13168, 2025.

Yang, Y., Nie, J., Miao, Y., Wan, S., and Jonell, T. N.: Tibetan Plateau uplift

https://doi.org/10.5194/egusphere-2025-5342
Preprint. Discussion started: 27 November 2025

and environmental impacts: New progress and perspectives, Front. Earth Sci., 10, 1020354, https://doi.org/10.3389/feart.2022.1020354, 2022.

Zeng, S., Wang, J., Fu, X., Feng, X., and Wang, D.: Controls on organic matter enrichment of the early-middle miocene lacustrine oil shale, central tibet (sw china): new insights from clay minerals and geochemistry, J. Asian Earth Sci., 262, 106007, https://doi.org/10.1016/j.jseaes.2024.106007, 2024.

Zhang, M., Guo, Z., Xu, S., Barry, P. H., Sano, Y., Zhang, L., Halldórsson, S. A., Chen, A., Cheng, Z., Liu, C., Li, S., Lang, Y., Zheng, G., Li, Z., Li, L., and Li, Y.: Linking deeply-sourced volatile emissions to plateau growth dynamics in southeastern Tibetan Plateau, Nat. Commun., 12, 4157, https://doi.org/10.1038/s41467-021-24415-y, 2021.

Zhang, R., Jiang, D., Zhang, C., and Zhang, Z.: Distinct effects of Tibetan Plateau growth and global cooling on the eastern and central Asian climates during the Cenozoic, Glob. Planet. Change, 218, 103969, https://doi.org/10.1016/j.gloplacha.2022.103969, 2022.

Zhang, Q., Zhang, J., Ma, C., Feng, Z., Tang, W., and Fang, X.: Tibetan plateau uplift changed the Asian climate and regulated its responses to orbital forcing during the late Eocene to early Miocene, J. Geophys. Res.-Atmos., 130, e2024JD042872, https://doi.org/10.1029/2024JD042872, 2025.

Zhao, Z., Lu, H., Wang, S., Li, H., Li, C., Liu, D., Pan, J., Zheng, Y., and Bai, M.: The Cenozoic multiple-stage uplift of the Qiangtang Terrane, Tibetan

https://doi.org/10.5194/egusphere-2025-5342
Preprint. Discussion started: 27 November 2025

plateau, Front. Earth Sci., 10, 818079, https://doi.org/10.3389/feart.2022.818079, 2022.

Zhou, K., Zhang, S., Yang, M., Lu, J., Gao, R., Tong, L., Yin, L., Zhang, P., Wang, W., Liu, H., Shao, L., Hilton, J.: Palaeoclimatic influence on lake palaeoenvironment and organic matter accumulation in the Middle Jurassic Shimengou formation (Qaidam basin, NW China), Geoenergy Sci. Eng., 233, 212581, https://doi.org/10.1016/j.geoen.2023.212581, 2024.

Zhu, Z., Chen, J. A., Zeng, Y., Li, H., Yan, H., and Ren, S.: Research on the carbon isotopic composition of organic matter from Lake Chenghai and Caohai Lake sediments, Chin. J. Geochem., 30, 107-113, https://doi.org/10.1007/s11631-011-0491-9, 2011.

Zhu, Z., Chen, J., Zeng, Y.: Abnormal positive $\delta^{13}C$ values of carbonate in Lake Caohai, southwest China, and their possible relation to lower temperature, Quat. Int., 286, 85-93, https://doi.org/10.1016/j.quaint.2012.06.004, 2013.

Zhuang, Q., Guo, M., Melack, J. M., Lan, X., Tan, Z., Oh, Y., and Leung, L. R.: Current and future global lake methane emissions: A process-based modeling analysis, J. Geophys. Res-biogeo., 128, e2022JG007137, https://doi.org/10.1029/2022JG007137, 2023.